

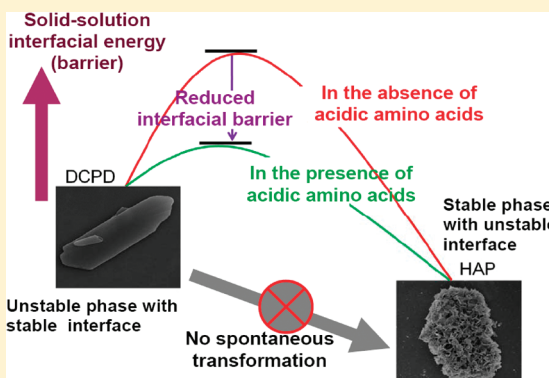
Unique Roles of Acidic Amino Acids in Phase Transformation of Calcium Phosphates

Xiaobin Chu, Wenge Jiang, Zhisen Zhang, Yang Yan, Haihua Pan, Xurong Xu,* and Ruikang Tang*

Center for Biomaterials and Biopathways and Department of Chemistry, Zhejiang University, Hangzhou, Zhejiang, 310027, China

 Supporting Information

ABSTRACT: Although phase transformation is suggested as a key step in biominerization, the chemical scenario about how organic molecules mediate inorganic phase transformations is still unclear. The inhibitory effect of amino acids on hydroxyapatite (HAP, the main inorganic component of biological hard tissues such as bone and enamel) formation was concluded by the previous biomimetic modeling based upon direct solution crystallization. Here we demonstrate that acidic amino acids, Asp and Glu, could promote HAP crystallization from its precursor crystal, brushite (DCPD). However, such a promotion effect could not be observed when the nonacidic amino acids were applied in the transformation-based HAP formation. We found that the specific modification of acidic amino acid on crystal–solution interfaces played a key role in the phase transition. The distinct properties between DCPD and HAP in the solution resulted in an interfacial energy barrier to suppress the spontaneous formation of HAP phase on DCPD phase. Different from the other amino acids, the carboxylate-rich amino acids, Asp and Glu, could modify the interfacial characteristics of these two calcium phosphate crystals to make them similar to each other. The experiments confirmed that the involvement of Asp or Glu reduced the interfacial energy barrier between DCPD and HAP, leading to a trigger effect on the phase transformation. An in-depth understanding about the unique roles of acidic amino acids may contribute to understanding phase transformation controls during biominerization.



1. INTRODUCTION

It is widely accepted that enrollment of biomolecules is key to biominerization controls.¹ Physiochemical modeling of the regulations has attracted considerable attention due to its implications in various fields ranging from chemistry to material and biology sciences.² People believe that the constructive interactions between inorganic phase and organic matrix (especially proteins) deterministically mediate nucleation, growth kinetics, and facet stability of minerals.^{3–5} Specific protein functional groups provide suitable heterogeneous nucleation sites to induce mineralization reactions.⁶ However, numerous biomimetic studies about crystallization kinetics in the presence of organic additives including the biominerization proteins have revealed that such organic–inorganic interactions in fact result in inhibition and even suppression of mineral formation.^{7,8} We note that the previous understanding about biominerization is frequently established upon a classic model of solution crystallization, suggesting that mineral crystals are produced directly from solution ions under supersaturated conditions.⁹ However, this classic model was recently challenged by a multistep mechanism of biominerization,^{10–12} which emphasizes that transient phases precipitate first prior to final crystal formation in biominerization. For example, the common biomineral crystallites such as hydroxyapatite (HAP, $\text{Ca}_{10}(\text{PO}_4)_6(\text{OH})_2$) and calcite

are not one-step generated in living organisms.^{12,13} More and more evidence shows that the final mineral products are transformed from their pre-existing interim solid states such as amorphous calcium phosphate (ACP) and amorphous calcium carbonates (ACC).¹⁴ The mineralization pathway via intermediate states involves a minimum energy barrier, which is significantly lower than that from the direct crystallization.¹⁵ Such a feature is highly advantageous to produce minerals under mild biological conditions.¹⁶ During the biological apatite mineralization or bone regenerations, *in vivo* phase transformation from ACP, brushite (DCPD, $\text{CaHPO}_4 \cdot 2\text{H}_2\text{O}$), tricalcium phosphate (TCP, $\text{Ca}_3(\text{PO}_4)_2$), and octacalcium phosphate (OCP, $\text{Ca}_8\text{H}_2(\text{PO}_4)_6 \cdot 5\text{H}_2\text{O}$) to HAP has been observed.^{10,17}

The chemical scenario about how biomolecules mediate phase transformations is unclear.¹⁸ Our latest achievement has revealed that Asp can accelerate phase transformation of calcium minerals from their magnesium-stabilized amorphous precursors.¹⁹ In this paper, we demonstrate that the acidic amino acids, Asp and Glu, promote HAP formation from its precursor crystal, DCPD, effectively. It is assumed that such a promotion effect is not

Received: July 23, 2010

Revised: December 6, 2010

Published: December 29, 2010

achieved by using any nonacidic amino acids. These abnormal phenomena cannot be understood by the influences of different amino acids on independent HAP crystallization or DCPD dissolution. We note that the distinct surface properties of DCPD and HAP in the reaction solution actually result in an interfacial barrier during the phase transition. However, Asp and Glu can make the two interfaces similar to each other so that the barrier can be reduced. Thus, the Asp- or Glu-modified DCPD—solution interfaces can induce HAP formation more readily. The computer simulation results, in conjunction with the interfacial examination, suggest that the carboxylate-rich feature of Asp and Glu is critical in the selective modification. Interestingly, the proteins which are most active in the mediation of mineralization always contain a high content of acidic amino acid residues and are also carboxylate rich.²⁰

2. EXPERIMENTAL SECTION

2.1. Materials. DCPD crystals were prepared in our laboratory according to the Marshall method.²¹ Amino acids were purchased from Sigma-Aldrich (USA); other reagents (analysis grade) were purchased from Sinopharm Chemical Reagent Co. Ltd. (China). No additional purification was applied. Triply distilled water was used, and all solutions were filtered by 0.22 μm Millipore membranes prior to use.

2.2. Phase Transformation. All experiments were performed at a room temperature of 25 °C. The reaction solution contained 10 mM sodium phosphate, and the ionic strength, I , was fixed at 0.15 M using sodium chloride. The amino acid component was added into the solution prior to pH adjustment. The solution pH was adjusted to 8.45 ± 0.02 using 0.01 M sodium hydroxide or hydrochloric acid. A 50 mg amount of DCPD seeds was exposed to 100 mL of reaction solution to start the experiment. The suspension was magnetically stirred at 300 rpm. The solids were withdrawn periodically by filtration, washed with water, and dried in a vacuum.

2.3. Characterization. XRD was examined using a D8-Advance (Bruker, Germany) with Cu K α radiation ($\lambda = 1.540 \text{ \AA}$, Ni filter). Scanning electron microscopy (SEM) was performed by a S-4000 (Hitachi, Japan). The FT-IR spectra were collected from 4000 to 400 cm^{-1} in the transmission mode by a Nexus-670 spectrometer (Nicolet, USA).

2.4. Constant Composition (CC).²² This method could be used to mimic the biologically stabilized solution conditions during mineralization or demineralization. The reaction solutions (100 mL) were prepared by mixing calcium chloride and potassium dihydrogen phosphate with sodium chloride to maintain $I = 0.15 \text{ M}$. pH was adjusted to the desired value. The amino acids were added prior to pH adjustment. Growth or dissolution was initiated by introduction of 20 mg of seed crystallites. The titrant addition was potentiometrically controlled by glass and Ag/AgCl reference electrodes. More experimental details can be found in the published literature.²² In order to understand the possible influence of DCPD substrate on HAP heterogeneous nucleation, 20 mg of DCPD or amino-acid-modified DCPD crystals was added into the HAP supersaturated solutions to examine the induction time period.

2.5. Atomic Force Microscopy (AFM). Images were collected using tapping mode using a DI Nano IVa instrument (Veeco, USA). The tip—surface interaction was reduced using the lowest tip force to ensure that the images were authentic representations of the surfaces.

2.6. Interfacial Energy²³. Briefly, the sessile drop method was used for the contact angle measurements with an OCA15+ instrument (Dataphysics, Germany). The interfacial energy, γ , was calculated by Young's equation using the parameters of solids and liquids. The unknown components of the calcium phosphates and solutions were obtained using the known parameters of probing liquids and probing substrates (see Supporting Information) using eq 1

$$(1 + \cos \theta) \gamma_L = 2 \left(\sqrt{\gamma_S^{\text{LW}} / \gamma_L^{\text{LW}}} + \sqrt{\gamma_S^+ \gamma_L^-} + \sqrt{\gamma_S^- \gamma_L^+} \right) \quad (1)$$

where θ is the measured contact angle, subscripts S and L represent the solid surface and test liquids, respectively, γ^{LW} is the Lifshitz–van der Walls (or apolar) surface tension component, γ^+ the Lewis acid (electron-acceptor) parameter, and γ^- the Lewis base (electron-donor) parameter. The interfacial energy between the crystal and solutions, γ_{SL} , was calculated using eq 2

$$\gamma_{SL} = \left(\sqrt{\gamma_S^{\text{LW}} - \gamma_L^{\text{LW}}} \right)^2 + 2 \left(\sqrt{\gamma_S^+ \gamma_S^-} + \sqrt{\gamma_L^+ \gamma_L^-} - \sqrt{\gamma_S^+ \gamma_L^-} - \sqrt{\gamma_S^- \gamma_L^+} \right) \quad (2)$$

2.7. Computer Simulation.²⁴ Briefly, the HAP (100) and DCPD (010) faces were used in the simulation. Molecular dynamic (MD) simulations were performed using a Gromacs 3.3 package, and the details are described in ref 24. The AFM pulling method was used to calculate the potential of the adsorption of amino acids on the minerals using Jarzynski's equality.²⁵

3. RESULTS AND DISCUSSION

Since amino acids are the basic protein constituents, their roles in biomimetic mineralization have been extensively examined.²⁶ Crystallization kinetics of HAP in the presence of various amino acids has already been studied, and the inhibitory effect is commonly concluded.^{27,28} In our studies, six typical amino acids, Gly, Ala, Ser, Asp, Glu, and His, were selected for a systematic study. CC experiments confirmed that all these amino acids retarded the crystal growth of HAP from its supersaturated solutions (Figure 1). The retardant effects of the acidic ones, Asp and Glu, were more significant than the others. However, the HAP formation from DCPD precursor phase was promoted significantly in the presence of Asp and Glu (Figure 2a). Clearly, this promotion effect was opposite to the inhibitory effect derived from the direct solution crystallization model. Among calcium phosphates, HAP is the most thermodynamically stable under basic conditions. It is generally considered that the transformation from the relatively unstable DCPD to HAP is spontaneous in basic solution (our experimental condition was pH = 8.45). Different from expectation, our study showed that the reaction was extremely slow in the absence of any additives. In our experiments, no HAP formation was detected by X-ray diffraction (XRD) within 144 h. The phase of DCPD was unchanged in basic solution. Only partial dissolution of the crystals was observed under SEM (Figure 2b). The corresponding energy-dispersive spectrum (EDS) showed that the Ca:P ratio of the remaining solids was 1.03 ± 0.02 , indicating the persistence of

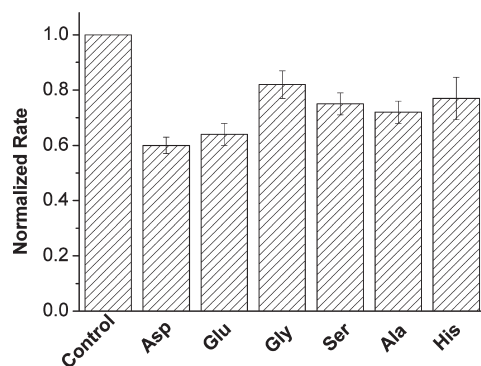


Figure 1. Normalized HAP crystal growth in the absence and presence of amino acids (0.2 mM) in a supersaturated solution (Ca = 0.5 mM, phosphate = 0.3 mM, pH = 7.4, ionic strength = 0.15 M).

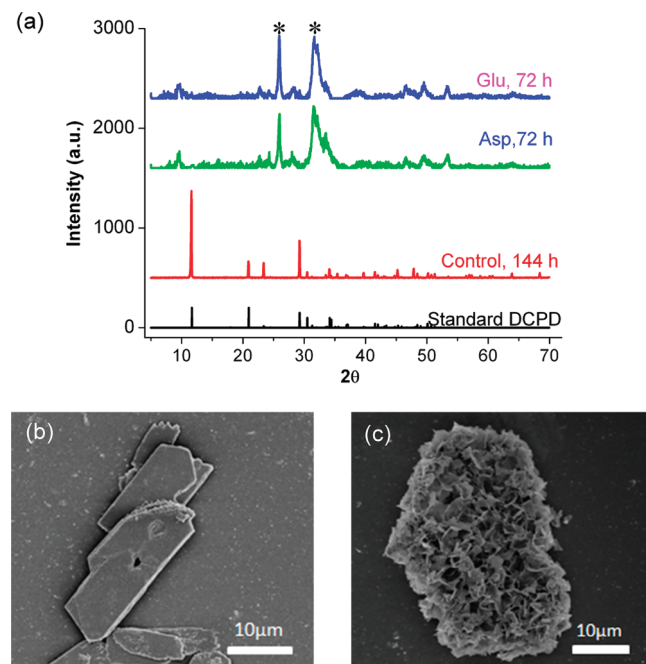


Figure 2. (a) XRD patterns of the solid samples in the absence and presence of acidic amino acids; the concentrations of Asp and Glu were 0.20 mM; the asterisks (*) indicate the diffraction peaks of HAP. SEM images of the solids at the end of experiments in the absence (b) and presence (c) of 0.2 mM Asp.

DCPD. In our previous study,²⁹ we found that a high interfacial barrier between DCPD–solution (0.20 mJ/m²) and HAP–solution (9.0 mJ/m²) made the transformation become kinetically unfavorable. In order to overcome the barrier, extra energy was required to start the evolution from the DCPD–solution interface to the HAP–solution interface. An alternative strategy to trigger the reaction was to lower the barrier using functional additives.

When 0.2 mM Asp was added (the solution pH was kept at 8.45), the signals of HAP appeared in the XRD spectrum within 48 h and the transformation could be completed within 72 h. The morphology changes of the crystals were observed during the reaction (Figure 2c). Numerous nanoflake-like crystals were found at the end of experiments, and the typical DCPD crystallite could not be found any more (Figure 2d). EDS results indicated

Table 1. Different Amino Acids (0.2 mM) and Their Roles in Transformation-Based HAP Formation from DCPD Precursor

amino acid	pI	transformation completion
Asp	2.77	≤72 h
Glu	3.22	≤72 h
Gly	5.97	no transformation
Ala	6.02	no transformation
Ser	5.68	no transformation
His	7.59	no transformation

that the Ca:P ratio of these newly formed crystallites was 1.61 ± 0.03 , agreeing with the HAP stoichiometry. Clearly, the involvement of Asp triggered the phase transformation from DCPD to HAP. By using Glu, a similar promotion effect was observed (Figure 2a). However, it was surprised that no transformation was observed when the other amino acids, Gly, Ala, Ser, and His, were applied as the regulators. The results of the phase transformation and isoelectric points (pI) of the used amino acids are summarized in Table 1. We noticed that only the acidic ones had a promotion effect on the calcium phosphate transformation. Besides, the supplementary experiments found that the other nonacidic amino acids such as Leu, Phe, Trp, Thr, Asn, and Arg were also inert in the crystal transformations.

According to the standard joint committee of powder diffraction spectra (JCPDS), the most intensive peaks of DCPD (09-0077) and HAP (09-0432) were detected at 2θ of 11.7° and 31.8°, respectively (Figure 3a). The intensities of these two typical peaks could be used to estimate the reaction kinetics semiquantitatively. The transformation degree, R , is defined by eq 3³⁰

$$R = \frac{I_{\text{HAP}}}{I_{\text{HAP}} + I_{\text{DCPD}}} \quad (3)$$

where I_{HAP} and I_{DCPD} were the intensities of the peaks at 2θ of 11.7° and 31.8°, respectively, in the XRD profiles. The plot of R vs time (Figure 3b) showed that the transformation kinetics could be enhanced by increasing Asp concentrations. At low concentration of 0.05 mM, the reaction started at around 96 h and was completed within 120 h. However, these two time periods were decreased to 60 and 84 h, respectively, when Asp amount was increased to 0.10 mM. The maximum promotion effect was achieved at a Asp concentration of 0.20 mM; further increases did not accelerate the reaction any more. The Asp concentration-dependent promotion tendency was confirmed independently by using FT-IR methods (see Supporting Information), and a similar behavior was achieved using Glu (Figure 4). However, even the concentrations of Gly, Ala, Ser, and His were raised to tens of millimolar; no phase transformation was detected, confirming the inert roles of nonacidic amino acids in the reaction. It was important to note that in the previous solution crystallization model an increase of organic additives including Asp frequently resulted in a more significant inhibitory effect on mineral formation. However, the active organic matrix actually benefits biomineralization in nature.³¹ Our result implied that the higher content of organic additives might promote the phase transformation kinetics more effectively.

The detailed mechanism in the calcium phosphate phase transformation is still equivocal despite intensive efforts. Many studies proposed that dissolution of precursor phase (DCPD) and recrystallization of the final product (HAP) were responsible

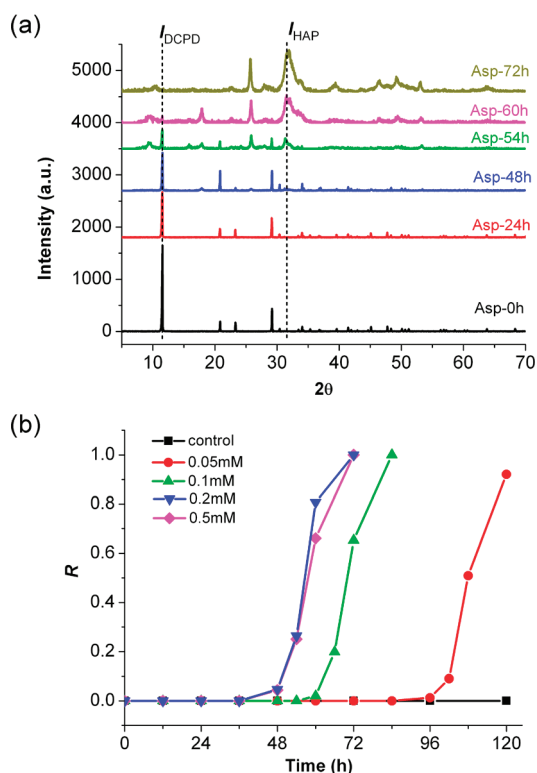


Figure 3. (a) XRD patterns of the solid samples at different experimental stages; the concentrations of Asp were 0.20 mM. (b) Kinetic plots of the phase transformation from DCPD to HAP in the presence of different Asp concentrations.

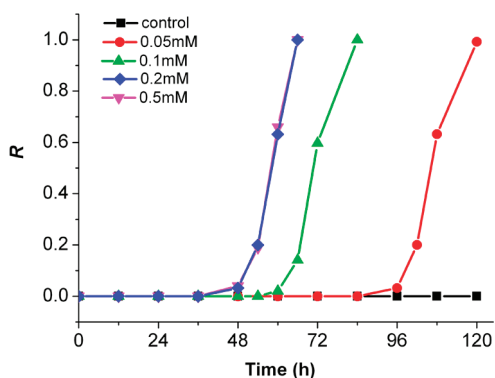


Figure 4. Kinetic plots of the phase transformation from DCPD to HAP in the presence of different Glu concentrations.

for the phase transformation.³² It suggested that the dissolution of DCPD and crystallization of HAP were two control steps. Thus, it was reasonable to expect that the acidic amino acids altered the dissolution behavior of DCPD or the crystallization of HAP. Unfortunately, it was demonstrated that these additives in fact inhibited the HAP crystal growth (Figure 1).^{8,26} We also investigated the influences of different amino acids on DCPD dissolution using CC. Again, all the amino acids inhibited the dissolution, and the order of inhibition was Gly > Asp > Glu > Ala > His > Ser. It seemed that the unique effect of Asp and Glu on the transformation promotion from DCPD to HAP could be explained by neither HAP crystallization nor DCPD dissolution modeling.

During the phase transformation, formation of HAP on DCPD was a critical step. We suggested that the acid amino acids could alter the interfacial compatibility of the calcium phosphate phases in the reaction solutions. It is well known that DCPD could be stable in air, and the aqueous medium was required for the transformation. The reaction occurred at the solid–liquid interface, and thereby, the interfacial structure between the solid and the solution must be taken into account. During the phase transformation, the interfacial Gibbs free energy change (ΔG_S) is expressed by

$$\Delta G_S = S_{\text{HAP}} \gamma_{\text{HAP}} - S_{\text{DCPD}} \gamma_{\text{DCPD}} \quad (4)$$

where S is the surface area of the crystals and γ is the interfacial energy between the solid and the reaction solution. In our experiment, the DCPD–solution interface turned into the HAP–solution interface during the transition. The interfacial energies between the solid and the reaction solution were calculated using a combination of Young's equation and contact angle measurement. The data showed that the interface of HAP–solution was distinct from that of DCPD–solution (Table 2). The examined contact angles of the reaction solution on HAP and DCPD were $42.1 \pm 1.5^\circ$ and $14.2 \pm 1.4^\circ$, respectively. The estimated γ_{HAP} , 9.00 mJ/m^2 , was greater than γ_{DCPD} , 0.20 mJ/m^2 . The difference of γ indicated that the DCPD surface was more stable than the HAP surface in the solutions. As a result, an extra energy was needed to turn the stable DCPD–solution interface into the unstable HAP–solution interface. The transition actually was thermodynamically unfavored at the solid–liquid interface. It was worse that the resulting HAP tiny crystallites had much greater surface areas than the relatively large DCPD seed crystals. Thus, ΔG_S was a greatly positive item, and this interfacial energy barrier must be lowered; otherwise, the reaction was kinetically suppressed at the interfaces. We mentioned that among the calcium minerals, the most stable phases always are characterized by their relatively high solid–liquid interfacial energy in solution.³³ Therefore, the interfacial energy barriers might hold generally in phase transformation.

The acidic amino acids could alter the interfacial properties of HAP and DCPD diversely. It is interesting that the solid–solution interfacial properties of HAP and DCPD became close to each other in the presence of acidic amino acids. This change could be represented by the contact angle measurements (see Table 2 and the Supporting Information). In the presence of 0.2 mM Asp, the contact angles of the reaction solutions on HAP and DCPD were reduced to $26.6 \pm 1.4^\circ$ and increased to $18.1 \pm 1.3^\circ$, respectively. Accordingly, the barrier between γ_{HAP} (5.83 mJ/m^2) and γ_{DCPD} (1.72 mJ/m^2) was reduced remarkably. The involvement of Asp resulted in a more stable HAP–solution interface and more active (unstable) DCPD–solution interface. Such opposite modification effects made the transition become more readily due to the reduced barrier. It could be seen that the induction time period in the phase transformation experiment was greatly shortened by Asp. Besides, the use of Glu resulted in the analogous effect to lower the interfacial energy barrier. In contrast, the modifications of the nonacidic amino acids on the calcium phosphate minerals were relatively weak and the changes insufficient. Table 2 shows that the influences of Gly, Ala, Ser, and His on DCPD–solution interfaces were negligible, and thus, their effects on HAP–solution interfaces were relatively limited. It could be noted that the contact angle changes by the nonacidic

Table 2. Measured Contact Angles and Calculated Interfacial Energies of DCPD and HAP in the Solutions^a

amino acid	DCPD		HAP		$\Delta\gamma$
	contact angle	γ_{DCPD} (mJ/m ²)	contact angle	γ_{HAP} (mJ/m ²)	
control	14.2 ± 1.4	0.20	42.1 ± 1.5	9.00	8.80
Asp	18.4 ± 1.3	1.72	26.4 ± 1.3	5.83	4.11
Glu	18.1 ± 1.3	1.72	26.6 ± 1.4	5.83	4.11
Gly	14.3 ± 1.3	0.20	39.6 ± 1.6	8.06	7.96
Ala	14.2 ± 1.3	0.20	41.0 ± 1.5	8.68	8.46
Ser	14.2 ± 1.2	0.20	37.6 ± 1.6	7.50	7.30
His	14.0 ± 1.5	0.20	38.4 ± 1.5	7.76	7.56

^a The probing solution was the same as that in the phase transformation experiment; the concentration of amino acid was 0.20 mM.

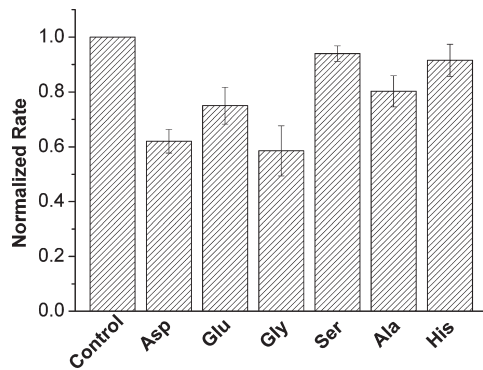


Figure 5. Normalized CC dissolution rates of DCPD in the absence and presence of different amino acids (0.2 mM) in an undersaturated solution ($\text{Ca} = 2.00 \text{ mM}$, phosphate = 2.00 mM, pH = 5.60, ionic strength = 0.15 M).

amino acids was always less than 5°, but Asp and Glu reduced the contact angles by about 16°.

The improved similarity between the HAP and the DCPD properties in the reaction solution contributed to HAP formation on the DCPD surface. In the CC study about HAP nucleation (the concentrations of calcium and phosphate ions were increased to 2.0 and 1.5 mM to facilitate reaction within a relatively short time period), it was found that pure DCPD actually had a poor influence on the induction time (Figure 6a). Usually, spontaneous crystallization occurs in bulk until critical conditions were reached or the driving force (supersaturation) was sufficiently high. Rather, a metastable equilibrium condition persisted during an induction period prior to crystal formation. If the simplifying assumption was made that the induction time was essentially concerned with classical nucleation, we could find that the nucleation rate was inversely proportional to the induction time. In the control, the homogeneous nucleation of HAP in solution was detected at an experimental time of 110 ± 5 min. Also, this induction time was almost unchanged, 108 ± 6 min, when DCPD seed was used as the substrate. This phenomenon implied that the DCPD–solution interface could not provide any active nucleation sites for HAP formation. AFM examination confirmed that HAP formation did not occur on DCPD substrate (Figure 6b). Only the typical dissolution pits were observed on DCPD when HAP nucleation was initiated. Clearly, the two interfacial properties of DCPD and HAP were not compatible with each other in the solutions, resulting in the weak interactions between the two calcium phosphate phases.

Amino acids alone in the solutions actually inhibited HAP nucleation (Figure 6c). The CC experiments demonstrated that all the amino acids including Asp and Glu resulted in longer induction time periods (127–336 min), agreeing with the conclusion from Figure 1. However, it was interesting that a combination of DCPD and amino acids could change the tendency. The DCPD crystals were treated in Asp and Glu solutions before use. Their surfaces were adsorbed and modified by the amino acids. The induction time of HAP nucleation in the supersaturated solution was reduced when these modified DCPD crystals were used as the substrates (Figure 6a). Different from the experiments represented by Figure 6c, the amino acids were immobilized on DCPD and resulted in the promotion effect on HAP formation. The AFM study revealed that the HAP was generated on the Asp pretreated DCPD surfaces (Figure 6d), confirming that the modified DCPD–solution interfaces provided the effective HAP heterogeneous nucleation sites. However, the DCPD crystals treated by the nonacidic amino acids did not exhibit this promotion effect. These experimental results demonstrated the importance of structural compatibility in phase generation at solid–solution interfaces.

The different modification effect of the amino acids on the solid–liquid interfaces of DCPD and HAP was understood by their adsorption behaviors. MD simulation was a useful tool for modeling and probing the structure and adsorption of organic molecules on inorganic crystals.^{34–36} The results showed that both carboxylate groups of Asp and Glu were involved in the adsorption on the calcium mineral facets. Their adsorptions were much stronger than the nonacidic amino acids, which had only one carboxylate group. The calculated adsorption free energy values of Asp on HAP and DCPD were -384 ± 55 and $-225 \pm 36 \text{ kJ/mol}$, respectively, and those of Glu on HAP and DCPD were -326 ± 29 and $-239 \pm 38 \text{ kJ/mol}$, respectively. In contrast, the corresponding values of the selected nonacidic amino acids were in the ranges from -250 to -200 and -160 to -100 kJ/mol , respectively. The absolute values were significantly lower than the corresponding ones of Asp and Glu. Thus, the strong adsorption abilities of Asp and Glu on the calcium phosphate minerals led to effective modifications of the interfacial properties.

In nature, although many extracted proteins associated with mineralized tissue are quite different with species, a common feature is that they contain many acidic moieties and are rich in Asp and Glu.^{37,38} For example, an acidic matrix protein, Aspein, has a pivotal role in shell mineralization. This protein is rich in Asp with a content of 60%. Besides, osteocalcin is a key protein in bone generation, and its characteristic amino acid composition is

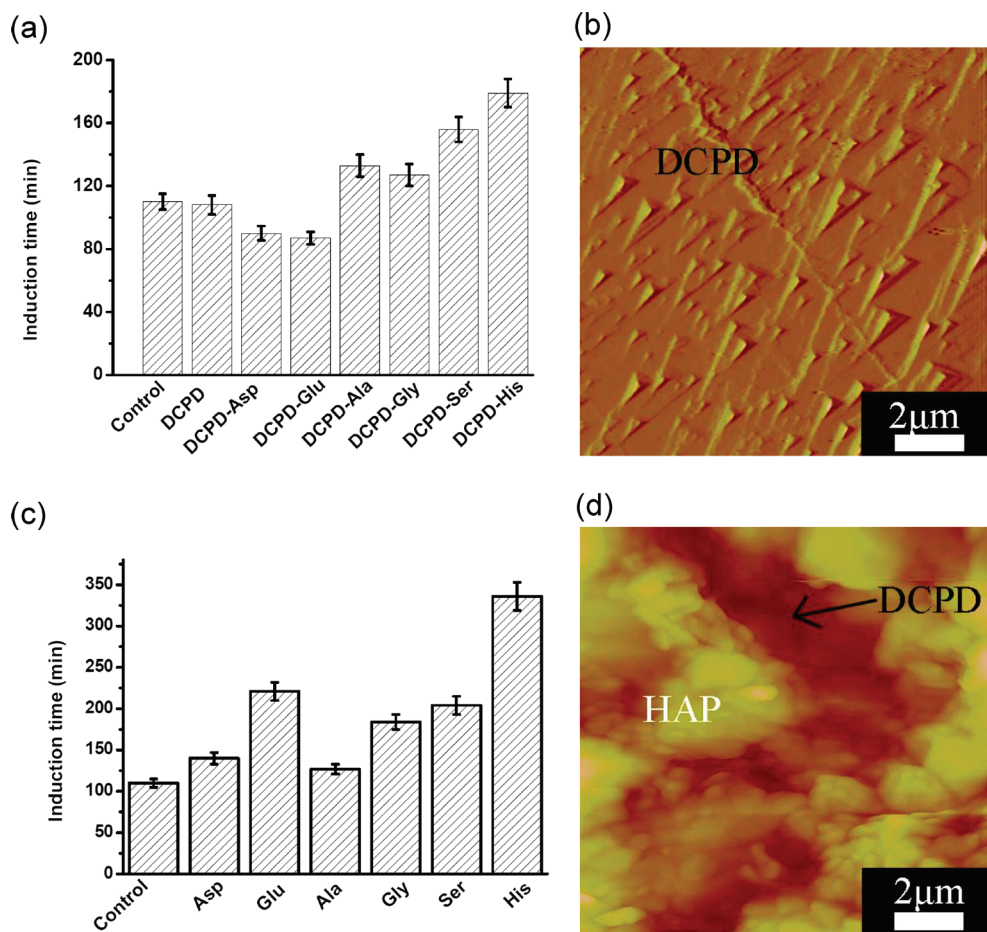


Figure 6. (a) Induction time of HAP nucleation in the absence and presence of different DCPD substrates ($\text{Ca} = 2.00 \text{ mM}$, phosphate = 1.50 mM , pH = 8.45, $I = 0.15 \text{ M}$); it should be noted that the amino acids were immobilized on the DCPD surfaces. (b) In situ AFM image of the DCPD crystal surface when the HAP nucleation was initiated in the solution. (c) Induction time of HAP nucleation in different amino acid solution; it should be noted that the amino acids were free in the solution. (d) Large-scale formation of HAP on the Asp-modified DCPD surface was observed by in situ AFM.

a highly acidic sequence consisting of consecutive Asp residues. Many studies have suggested that Asp and Glu together comprise more than 25 mol % of the constituent amino acids in the active biominerization proteins, which can promote hard tissue generations. The Asp and Glu residues actually confer carboxylate-rich domains on proteins. In biominerization, these domains provide the active sites to induce the calcium phosphate or calcium carbonate formations for the living organisms.³⁹ It is also noted that the content percentages of a number of nonacidic amino acids such as Gly, Ala, and Ser in the biominerization proteins are relatively high.^{36,40} Although these amino acids themselves are inert in the crystal transition and biominerization, they play a structural role to ensure the optimum effect of the “active sites” (carboxylate-rich domains). It is suggested that polypeptide should be an excellent model system to simulate proteins.⁴¹ However, Weiner, Cusack, and co-workers pointed that in the “active sites” of biominerization proteins, runs of acidic residues are commonly separated by Gly, Ala, or Ser.^{42,43} The acidic residues in an acidic block of protein are usually between 1 and 10 units, and short polypeptide may be more common.⁴³ The long chain poly-Asp and poly-Glu are in fact distinct from the biominerization protein; they cannot be considered as a suitable model for the biominerization proteins. It has been confirmed experimentally that the short poly-Asp

segments have a similar role with Asp monomer in the biomimetic studies despite the fact that the efficiencies may be different.⁴⁴ Actually, the carboxylate density and the chemical structure in these active segments are similar to those in the acidic amino acids or some small carboxylate-rich molecules, e.g., citrate. As a result, these molecules including citrate exhibit the same interfacial modification and promotion effects on the crystallization of HAP from DCPD.²⁹

4. CONCLUSIONS

The current work demonstrates the trigger and promotion effects of acidic amino acids on the crystal transition from DCPD to HAP, while the other amino acids do not have such functions. We find that the interfacial energetic control is key to control; acidic amino acids, Asp and Glu, can decrease the interfacial energy barrier significantly and induce the HAP formation on DCPD. A cooperative effect of acidic amino acids and DCPD substrates is highlighted in the biological regulation of mineralization. However, the regulation effects of the nonacidic amino acids are relatively poor, so that they cannot promote the transition. Coincidentally, the biominerization of active proteins always contains a high content of the acidic amino acid residues, which are carboxylate rich. Thus, we suggest that the unique roles

of the carboxylate-rich structure in the phase-transformation-based crystallization may be used to discover biominerization secrets.

■ ASSOCIATED CONTENT

S Supporting Information. Details of FT-IR, EDS, and interfacial energy studies; FT-IR spectra of the phase transformation from DCPD into HAP (Figure S1), and the peaks analyzed using the PeakFit program (Figure S2); Ca/P ratio variation with the experimental time (Figure S3); tables of the surface tension components used in the calculations of interfacial energy (Table S1) and the measured contact angles and calculated interfacial energies (Table S2). This material is available free of charge via the Internet at <http://pubs.acs.org>.

■ AUTHOR INFORMATION

Corresponding Author

*Phone/Fax: +86-571-87953736. E-mail: xrxu@zju.edu.cn; rtang@zju.edu.cn.

■ ACKNOWLEDGMENT

This work was supported by the Fundamental Research Funds for the Central Universities (KYJD09031), National Natural Science Foundation of China (20871102), Zhejiang Provincial Natural Science Foundation (R407087), and Daming Biominer-alization Foundation.

■ REFERENCES

- (1) Berman, A.; Addadi, L.; Weiner, S. *Nature* **1988**, *331*, 546.
- (2) (a) Weiner, S.; Addadi, L. *J. Mater. Chem.* **1997**, *7*, 689.
(b) Stupp, S. I.; Braun, P. V. *Science* **1997**, *277*, 1242.
- (3) Mann, S.; Archibald, D. D.; Didymus, J. M.; Douglas, T.; Heywood, B. R.; Meldrum, F. C.; Reeves, N. J. *Science* **1993**, *261*, 1286.
- (4) Teng, H. H.; Dove, P. M.; Orme, C. A.; De Yoreo, J. J. *Science* **1998**, *282*, 724.
- (5) Alivisatos, A. P. *Science* **2000**, *289*, 736.
- (6) Fu, G.; Qiu, S. R.; Orme, C. A.; Morse, D. E.; De Yoreo, J. J. *Adv. Mater.* **2005**, *17*, 2678.
- (7) (a) Romberg, R. W.; Werness, P. G.; Riggs, B. L.; Mann, K. G. *Biochemistry* **1986**, *25*, 1176. (b) Worcester, E. M.; Blumenthal, S. S.; Beshensky, A. M.; Lewand, D. L. *J. Bone. Miner. Res.* **1992**, *7*, 1029.
- (8) Koutsopoulos, S.; Dalas, E. *J. Cryst. Growth* **2000**, *217*, 410.
- (9) Lowenstam, H. A.; Weiner, S. *On Biominerization*; Oxford University Press: Oxford, 1989.
- (10) Lowenstam, H. A.; Weiner, S. *Science* **1985**, *227*, 51.
- (11) Fritz, M.; Belcher, A. M.; Radmacher, M.; Walters, D. A.; Hansma, P. K.; Stucky, G. D.; Morse, D. E.; Mann, S. *Nature* **1994**, *371*, 49.
- (12) (a) Belcher, A. M.; Wu, X. H.; Christensen, R. J.; Hansma, P. K.; Stucky, G. D.; Morse, D. E. *Nature* **1996**, *381*, 56. (b) Tseng, Y. H.; Mou, C. Y.; Chan, J. C. C. *J. Am. Chem. Soc.* **2006**, *128*, 6909.
- (13) Politis, Y.; Arad, T.; Klein, E.; Weiner, S.; Addadi, L. *Science* **2004**, *306*, 1161.
- (14) Zhan, J. H.; Tseng, Y. H.; Chan, J. C. C.; Mou, C. Y. *Adv. Funct. Mater.* **2005**, *15*, 2005.
- (15) Liu, Y.; Nancollas, G. H. *J. Phys. Chem. B* **1997**, *101*, 3464.
- (16) (a) Colfen, H.; Mann, S. *Angew. Chem., Int. Ed.* **2003**, *42*, 2350.
(b) Weiner, S.; Traub, W. *FASEB J.* **1992**, *6*, 879.
- (17) Dorozhkin, S. V.; Epple, M. *Angew. Chem., Int. Ed.* **2002**, *41*, 3130.
- (18) Yamamoto, K.; Kumagai, H.; Fujii, T.; Yano, T. *Biosci. Biotechnol. Biochem.* **1993**, *57*, 1788.
- (19) Tao, J. H.; Zhou, D. M.; Zhang, Z. S.; Xu, X. R.; Tang, R. K. *Proc. Natl. Acad. Sci. U.S.A.* **2009**, *106*, 22096.
- (20) Oldberg, A.; Franzen, A.; Heinegard, D. *Proc. Natl. Acad. Sci. U.S.A.* **1986**, *83*, 8819.
- (21) Marshall, R. W.; Nancollas, G. H. *J. Phys. Chem.* **1969**, *73*, 3838.
- (22) (a) Tang, R. K.; Nancollas, G. H.; Orme, C. A. *J. Am. Chem. Soc.* **2001**, *123*, 5437. (b) Tang, R. K.; Darragh, M.; Orme, C. A.; Guan, X. Y.; Hoyer, J. R.; Nancollas, G. H. *Angew. Chem., Int. Ed.* **2005**, *44*, 3698.
- (23) (a) Shen, Q. *Langmuir* **2000**, *16*, 4394. (b) Van Oss, C. J.; Chaudhury, M. K.; Good, R. J. *Chem. Rev.* **1988**, *88*, 927.
- (24) Pan, H. H.; Tao, J. H.; Xu, X. R.; Tang, R. K. *Langmuir* **2007**, *23*, 8972.
- (25) Jarzynski, C. *Phys. Rev. Lett.* **1997**, *78*, 2690–2693.
- (26) Gordon, G. V.; Schumacher, H. R.; Gohel, V. *Rheumatology* **1984**, *11*, 681.
- (27) (a) Koutsopoulos, S.; Dalas, E. *Langmuir* **2000**, *16*, 6739.
(b) Koutsopoulos, S.; Dalas, E. *J. Cryst. Growth* **2000**, *216*, 443.
- (28) Kresak, M.; Moreno, E. C.; Zahradnik, R. T.; Hay, D. I. *J. Colloid Interface Sci.* **1977**, *59*, 283.
- (29) Jiang, W. G.; Chu, X. B.; Wang, B.; Pan, H. H.; Xu, X. R.; Tang, R. K. *J. Phys. Chem. B* **2009**, *113*, 10838.
- (30) Xie, J.; Riley, C.; Chittur, K. *J. Biomed. Mater. Res.* **2001**, *57*, 357.
- (31) Dickerson, M. B.; Sandhage, K. H.; Naik, R. R. *Chem. Rev.* **2008**, *108*, 4935.
- (32) (a) Boskey, A. L.; Posner, A. S. *J. Phys. Chem.* **1973**, *77*, 2313.
(b) Lazic, S. *J. Cryst. Growth* **1995**, *147*, 147.
- (33) Wu, W. J.; Nancollas, G. H. *Adv. Colloid Interface Sci.* **1999**, *79*, 229.
- (34) (a) Cooper, T. G.; de Leeuw, N. H. *Langmuir* **2004**, *20*, 3984.
(b) de Leeuw, N.; Mkhonto, D. *Chem. Mater.* **2003**, *15*, 1567.
- (35) Duffy, D. M.; Harding, J. H. *Langmuir* **2004**, *20*, 7630.
- (36) Weiner, S. *Calcif. Tissue Int.* **1979**, *29*, 163.
- (37) Tsukamoto, D.; Sarashina, I.; Endo, K. *Biochem. Biophys. Res. Commun.* **2004**, *320*, 1175.
- (38) (a) Flade, K.; Lau, C.; Mertig, M.; Pompe, W. *Chem. Mater.* **2001**, *13*, 3596. (b) Hoang, Q. Q.; Sicheri, F.; Howard, A. J.; Yang, D. S. C. *Nature* **2003**, *425*, 977.
- (39) Qiu, S. R.; Wierzbicki, A.; Orme, C. A.; Cody, A. M.; Hoyer, J. R.; Nancollas, G. H.; Zepeda, S.; De Yoreo, J. J. *Proc. Natl. Acad. Sci. U.S.A.* **2004**, *101*, 1811.
- (40) Elhadj, S.; Salter, E. A.; Wierzbicki, A.; De Yoreo, J. J.; Han, N.; Dove, P. M. *Cryst. Growth Des.* **2006**, *6*, 197.
- (41) (a) De Yoreo, J. J.; Wierzbicki, A.; Dove, P. M. *CrystEngComm* **2007**, *9*, 1144. (b) Lam, R. S. K.; Charnock, J. M.; Lennie, A.; Meldrum, F. C. *CrystEngComm* **2007**, *9*, 1226.
- (42) Weiner, S.; Hood, L. *Science* **1975**, *190*, 987.
- (43) Cusack, M.; Freer, A. *Chem. Rev.* **2008**, *108*, 4433.
- (44) Elhadj, S.; De Yoreo, J. J.; Hoyer, J. R.; Dove, P. M. *Proc. Natl. Acad. Sci. U.S.A.* **2006**, *103*, 19237.